Laser–radio-frequency double-resonance spectroscopy of $^{84-87}$Rb isotopes trapped in superfluid helium

Xiaofei Yang,[1,2,*] Takeshi Furukawa,[3] Takashi Wakui,[4] Tomomi Fujita,[5] Kei Imamura,[2,6] Yosuke Mitsuya,[6] Miki Hayasaka,[7] Yuichi Ichikawa,[2] Yoko Ishibashi,[2,8] Hazuki Shirai,[9] Takahiro Suzuki,[9] Yuta Ebara,[3] Atsushi Hatakeyama,[10] Michiharu Wada,[2] Tetsu Sonoda,[2] Yuta Ito,[2] Tohru Kobayashi,[11] Shunji Nishimura,[2] Mizuki Kurata-Nishimura,[2] Yosuke Kondo,[9] Ken-Ichiro Yoneda,[2] Shigeru Kubono,[2] Yoshimitsu Ohshiro,[12] Hideki Ueno,[2] Tsutomu Shinozuka,[4] Tadashi Shimoda,[5] Koichiro Asahi,[9] and Yukari Matsuo[2,13]

[1]*State Key Laboratory of Nuclear Physics and Technology, School of Physics, Peking University, Beijing 100871, China*
[2]*RIKEN Nishina Center, 2-1 Hirosawa, Wako, Saitama 351-0198, Japan*
[3]*Department of Physics, Tokyo Metropolitan University, 1-1 Minami-Osawa, Hachioji, Tokyo 192-0397, Japan*
[4]*Cyclotron Radioisotope Center, Tohoku University, 6-3 Aoba, Aramaki, Aoba-ku, Sendai, Miyagi, 980-8578, Japan*
[5]*Department of Physics, Osaka University, 1-1 Machikaneyama, Toyonaka, Osaka 560-0043, Japan*
[6]*Department of Physics, Meiji University, 1-1-1 Higashi-Mita, Tama-ku, Kawasaki, Kanagawa 214-8571, Japan*
[7]*Department of Physics, Tokyo Gakugei University, 4-1-1 Nukuikitamachi, Koganei, Tokyo 184-8501, Japan*
[8]*Department of Physics, University of Tsukuba, 1-1-1 Tennodai, Tsukuba, Ibaraki 305-8577, Japan*
[9]*Department of Physics, Tokyo Institute of Technology, 2-12-1 O-Okayama, Meguro, Tokyo 152-8551, Japan*
[10]*Department of Applied Physics, Tokyo University of Agriculture and Technology, 2-24-16 Naka-cho, Koganei, Tokyo 184-8588, Japan*
[11]*Laser Technology Laboratory, RIKEN Center for Advanced Photonics, 2-1 Hirosawa, Wako, Saitama 351-0198, Japan*
[12]*Center for Nuclear Study, The University of Tokyo, 2-1 Hirosawa, Wako, Saitama 351-0198, Japan*
[13]*Department of Advanced Sciences, Hosei University, 3-7-2 Kajino-cho, Koganei, Tokyo 184-8584, Japan*

(Received 15 March 2014; revised manuscript received 20 October 2014; published 19 November 2014)

In this paper, we report on a laser spectroscopy measurement of $^{84-87}$Rb isotopes in superfluid helium (He II) at 1.8 K using laser–radio-frequency double-resonance spectroscopy. Rb ion beams (>60 MeV/u) provided by the RIKEN projectile fragment separator (RIPS) were injected and trapped into He II. The stopping position of atoms in He II was precisely confirmed by laser spectroscopy. By optically pumping the trapped Rb isotopes, large atomic spin polarization (up to 40%) of each observed isotope in the ground state was achieved. The laser–radio-frequency double-resonance spectra were observed for stable ^{85,87}Rb isotopes as well as for unstable isotopes ^{84,84m,86}Rb by scanning a weak magnetic field with a fixed-frequency RF field. From the measured Zeeman splitting, nuclear spin values for $^{84m,84-87}$Rb isotopes were determined with reasonable accuracy. The number of ions injected into He II for the resonance spectra measurement was on the order of 10^4 particles per second. This work may open new opportunities for the study of various particles trapped in condensed helium in several fields.

DOI: 10.1103/PhysRevA.90.052516 PACS number(s): 32.30.−r, 32.80.Xx, 36.10.−k, 42.62.Fi

I. INTRODUCTION

The laser spectroscopy measurement of various impurities in the matrices of condensed helium has attracted a great deal of attention over many years. It has revealed numerous fascinating properties of both foreign particles and quantum matrices [1–4]. The properties of impurities (atoms, molecules, ions, electrons) in helium (superfluid helium, solid helium, nanodroplets, and so forth) can be applied not only to the study of atomic phenomena [5–8] but also to several fields of research [9–12] such as fundamental physics, spin properties, and quantum computing. Since the pioneering work on the optical pumping of atoms in superfluid helium (He II) by implanting atoms into He II by a laser sputtering method [5], laser spectroscopy measurements of various atomic species in a helium have been carried out intensively to clarify spectral and spin properties and to study magnetic resonance spectra [7,8,13,14].

Our interest in the laser spectroscopy measurement of various atomic species was sparked by the confirmation of the greatly broadened (10 nm) and blue-shifted (>15 nm) absorption line spectrum [15] of atoms and the successful optical pumping of Rb and Cs atoms in He II [14]. In recent years, our group has been studying spectral and spin properties for a variety of atomic species in He II [16,17]. The initial work by Furukawa *et al.* [13] confirmed the long relaxation time (>2 s) as well as the long residence time of Cs atoms in He II, which enabled us to obtain a deeper understanding of the spin relaxation mechanism and perform high-resolution magnetic resonance experiments. Subsequently, making use of the broadened absorption spectra and long spin relaxation time of atoms in He II, sufficiently large atomic and nuclear polarization was achieved by optical pumping of stable alkali-metal atoms (Rb, 50%; Cs, 90%) as well as non-alkali-metal atoms (Ag and Au, 85%) [18]. In addition, the Zeeman and hyperfine resonances [19] of stable Rb and Cs atoms in He II have been observed by combining optical pumping and double-resonance methods. These studies have also confirmed that the He II medium barely affects the sublevel structure of atoms [14,17], although it results in the markedly

*yangxf@ribf.riken.jp

broadened and blue-shifted excitation spectra of atoms [15].

The early studies on the atoms in He II have provided a number of valuable results, as described above. However, these studies have so far been limited to solid sample of stable isotopes [5]. Moreover, the number of atoms that must be implanted into He II for observation is quite large and cannot be accurately estimated. In this study, a breakthrough was achieved by implementing a method allowing laser spectroscopy studies of various atomic species in He II using a small and controllable number of atoms. In this method, energetic ions produced at a separator such as the RIKEN projectile fragment separator (RIPS) [20] are injected into He II. Therefore, almost all elements, regardless of whether they are in a solid, liquid, or gaseous state, can be introduced into He II, because the atoms are produced by a nuclear reaction that is independent of their chemical properties. The number of implanted atoms is fully controlled by counting the injected ions one by one using detectors, as described in Refs. [21,22]. The injected radioactive ions are readily neutralized during the implantation process and are trapped in He II for subsequent laser spectroscopy measurement.

Here, we report on the stopping, trapping, polarization, and laser spectroscopy measurement of $^{84-87}$Rb isotopes in He II. Both stable ^{85,87}Rb and unstable ^{84,86}Rb energetic ions produced by an accelerator were accurately counted and implanted into He II. The number of injected atoms used in the measurement was on the order of 10^4 pps for the current setup system. The precision of the trapping site of atoms in He II was confirmed by detecting laser-induced fluorescence (LIF). By optical pumping, relatively high spin polarization was achieved for the $^{84-87}$Rb isotopes. The successful observation of laser–radio-frequency double-resonance (LRDR) spectra for the stable isotopes (^{85,87}Rb), radioactive isotopes (^{84,86}Rb), and an isomer (^{84m}Rb) allowed us to determine their nuclear spins. In the present study, we investigate the possible applications of our technique in studying the atomic physics and nuclear physics of various isotopes trapped in He II.

This paper is organized as follows: First, the experimental setup and procedure for trapping and laser spectroscopy observation are described in Sec. II. Then, experimental results and a discussion are presented in Sec. III. Finally, an overview of the work is given in Sec. IV.

II. DESCRIPTION OF THE EXPERIMENT

A. Outline of the experimental procedure and setup

A general introduction to the experimental principle and method was presented in a recent article reporting a preliminary result for the stable ^{87}Rb isotope [23]. Basically, the experiment includes two steps: the trapping of ions produced from an in-flight radioactive isotope (RI) separator in He II, and the laser spectroscopy measurement of atoms confined in He II. This measurement is accomplished by achieving atomic polarization by optical pumping and observing the LRDR spectra of trapped atoms.

A schematic view of the present experimental system is shown in Fig. 1. Energetic ion beams produced by a projectile fragment separator are slowed by a discrete set of aluminum foils with different thicknesses, referred to as an energy degrader (Al-deg2). The total thickness of the Al-deg2 can be adjusted remotely from 0 to 800 μm in 12.5-μm steps. Before being injected into He II, the ions are counted by a plastic scintillator (PL1) (100-μm thickness) assembled with two photomultiplier tubes (PMTs) located inside the chamber in front of a cryostat. The stopping position of the injected beams in He II is preliminarily checked by another plastic scintillator (PL2) located at the center of the cryostat. The He II can be maintained under the same conditions in the inner chamber of the cryostat for a long time (up to one day using the current system) [24]. The temperature of He II is kept at approximately 1.8 K by controlling the pumping speed of evaporated helium gas and the filling rate of helium. The vacuum, air, and He II regions are highly isolated by Kapton foils (75-μm thickness). In the inner chamber of the cryostat,

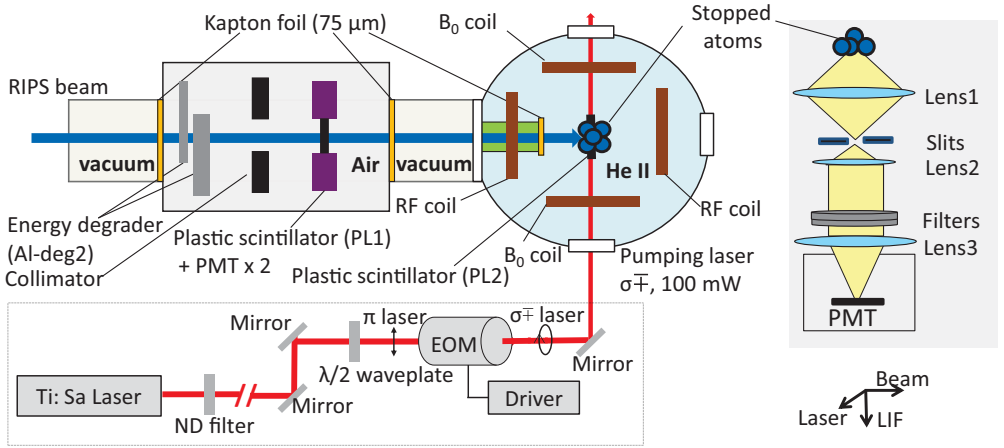

FIG. 1. (Color online) Schematic view of the experimental setup. Energetic ion beams produced by a projectile fragment separator are injected into the experimental setup. An energy degrader and the first plastic scintillator (PL1) are used to adjust the beam energy and count the injected ions, respectively. The second plastic scintillator (PL2) in the cryostat is used to check the stopping position of the beams in He II. The trapped atoms in He II are irradiated by circularly polarized laser light. Two sets of coils are used, one to apply a magnetic field B_0 and one to apply a RF field. The photon-detection system, as shown on the right, which detects the laser-induced fluorescence photons emitted from the laser-excited atoms, is located under the cryostat.

two pairs of coils are arrayed orthogonally. One set of coils (magnetic field coils, 10 turns, 30-mm diameter) is used to apply a magnetic field B_0 to obtain polarized atoms, while the other set (RF coils, 10 turns, 30-mm diameter) is used to supply an RF field required to observe LRDR spectra. The trapped atoms are excited by a continuous-wave (cw) pumping laser light (780-nm wavelength; approx. 100 mW of power adjusted by a neutral density (ND) filter; spot diameter: 2 mm). The laser light from a Ti:Sa laser (Coherent Co., Ltd., 899−01 Ti:sapphire laser) is circularly polarized by an electro-optic modulator (EOM, LM 0202; Qioptiq Photonics GmbH & Co. KG). Here, a $\lambda/2$ wave plate is used together with the EOM to switch the circularly polarized laser between σ^+ and σ^-. The LIF photons emitted from the laser-excited atoms (approx. 793-nm emission wavelength for Rb isotopes in He II) are collected by a photon-detection system [25] (shown on the right in Fig. 1) placed below the cryostat. This photon-detection system comprises three large Fresnel lenses, a pair of orthometric slits (parallel and perpendicular to the laser light) remotely controlled using a LabVIEW program, band-pass and edge-pass interference filters for perfect separation of the wavelengths, and a cooled PMT (Hamamatsu Co., Ltd., R943-02 and C10372).

B. Production and trapping of Rb isotopes

The experiments were performed at the RIPS separator of the RIKEN Radioactive Isotope Beam Factory (RIBF) [20]. The 66 MeV/u primary ^{85}Rb and ^{87}Rb beams accelerated by the RIKEN azimuthally varying field (AVF) cyclotron and the RIKEN ring cyclotron (RRC) propagated directly through the RIPS beam line with a set of suitable parameters such as magnetic rigidity, slit size, and so forth. Secondary ^{84}Rb and ^{86}Rb ion beams with an energy of 62 MeV/u were produced, respectively, by ^{85}Rb and ^{87}Rb beams impinging on a 125-μm Be target. The isotopes in the secondary beams are separated by the combined analyses of the magnetic rigidity and momentum loss in a curved degrader fabricated from an aluminum plate with an effective thickness of 43.50 mg/cm^2 and an equivalent wedge angle of 0.218 mrad. The thicknesses of the target and degrader were chosen on the basis of a LISE++ calculation [26], considering that the separated ion beams should have sufficient energy to be transported into He II. Both the primary beams and the isotope-separated beams were focused into the collimator located inside the chamber in front of the cryostat. The typical intensity for all the isotopes ($^{84-87}$Rb) was less than 10^5 pps.

To perform the optical pumping and LRDR spectroscopy measurement of atoms, it is particularly important to precisely trap the injected ions in the observation region of the laser in He II. In the present experiments, the energetic radioactive ions were continuously introduced and stopped in He II. The stopping position of Rb atoms in He II (approximately 7.5 mm from the injection window) was controlled by adjusting the energy of the ions via the thickness of the Al-deg2. The trapping position of atoms was preliminarily estimated by investigating the change in the count ratio between PL1 and PL2 with the Al-deg2 thickness. The perfect overlap between the laser beam and the trapped atoms was eventually confirmed by detecting the LIF photons emitted from the laser-excited atoms. Some earlier studies suggested that the energetic ions in He II can mostly be neutralized during the stopping process [11,27] and trapped easily for a long time (typically 0.5 s in our setup [23]) because of the high density of He II.

C. Observation of optical pumping and LRDR spectra of Rb isotopes

After trapping, the $^{84-87}$Rb atoms were then optically pumped and polarized with a circularly polarized laser light whose wavelength was tuned to the D_1 ($S_{1/2} \rightarrow P_{1/2}$) absorption line of Rb atoms (780 nm) in He II [15]. To achieve polarized atoms by the optical pumping method, a weak external magnetic field B_0 was applied to the trapped atoms in advance. During an optical pumping cycle, the excitation and emission of atoms follow the transition rules $\Delta m_F = +1$ (σ^+ pumping laser) and $\Delta m_F = \pm 1, 0$, respectively. Taking the ground-state energy level structure of ^{87}Rb as an example, as shown on the left side of Fig. 2(a), in the case of a σ^+ pumping laser, the atomic polarization is reflected by the population of the atomic state being concentrated at the

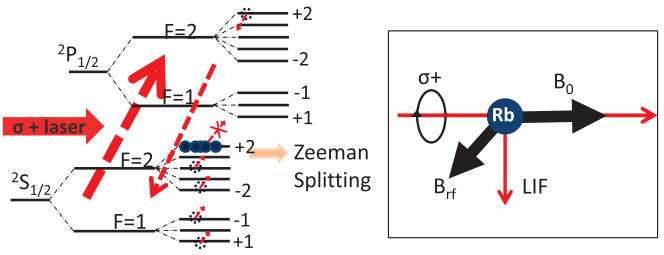

(a)

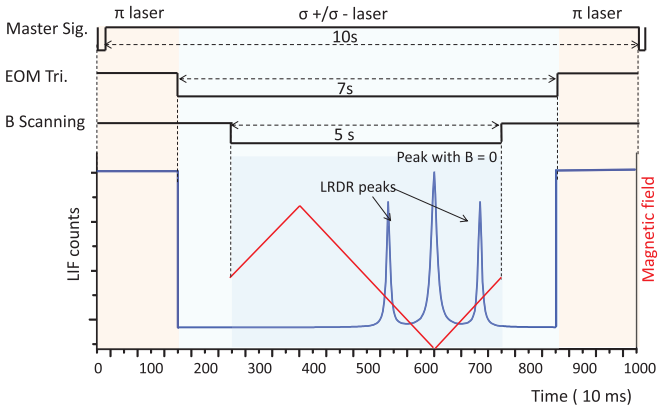

(b)

FIG. 2. (Color online) (a) (left) Schematic of optical pumping to achieve polarized atoms. Taking the ground-state energy level structure of ^{87}Rb as an example, the polarization of atoms is reflected by the population of the atomic states being concentrated at the maximum quantum number $m_F = +2$. (a) (right) Vector relation between propagation of the laser, applied magnetic field B_0, and RF field, and laser-induced fluorescence photons. (b) Block diagram showing measurement of LRDR spectra. The spectrum was recorded by scanning the magnetic field B_0 with a fixed RF field (1.8 MHz in the current spectrum) applied to the atoms.

maximum quantum number $m_F = +2$. Furthermore, owing to the forbidden transition, the pumping laser cannot be absorbed by the polarized atoms. The atoms are then depolarized, arising from the resonance transition between Zeeman levels induced by the applied RF field. All the optical pumping and LRDR processes can be recorded by detecting the LIF photons emitted from laser-excited atoms. The vector relation between the propagation of the laser, the applied magnetic field and RF field, and the detection of LIF photons is presented in the right panel of Fig. 2(a). The direction of the laser is parallel to the applied magnetic field B_0, whereas the RF field is perpendicular to both the magnetic field and the propagation direction of the laser.

In the experiment, LRDR spectra were measured by monitoring the LIF signal at 793 nm as a function of the scanned external magnetic field with a fixed-frequency transverse RF field applied to the atoms. Figure 2(b) shows the block diagram for the observation of the LRDR spectrum and the theoretically expected spectrum. The master signal, used to start the recording of spectra, is also the time reference used for the subsequent alternation of laser polarization and triggering of the scanning magnetic field and applied RF field. The pumping laser was alternated between linear and circular polarization by the EOM. The recorded LIF intensity is inversely related to the polarization of atoms during optical pumping, which is described as

$$I_{\mathrm{LIF}} \propto N_{\mathrm{atom}}(1 - \sigma P_z), \tag{1}$$

where N_{atom} is the number of atoms in the observation region, P_z is the polarization ratio of atoms, and σ is the polarization of the pumping laser. LRDR peaks, as marked in Fig. 2(b), are visible when the strength of the scanned magnetic field satisfies

$$\Delta E_z = K g_J \mu_B B_0, \tag{2}$$

where

$$K = \frac{F(F+1) + J(J+1) - I(I+1)}{2F(F+1)}.$$

In this equation, ΔE_z is the Zeeman splitting energy corresponding to the applied RF frequency, μ_B is the Bohr magneton, and g_J is the g factor. The nuclear g factor is negligible because of $\mu_N/\mu_B \propto \frac{m_e}{M_p} \sim 1/2000$ (m_e and M_p are the respective masses of an electron and nucleon). The resonance peak (B_0 peak) in the center of Fig. 2(b) appears when the applied scanning magnetic field is zero. This resonance can describe optical pumping with a circularly polarized laser in longitudinal and transverse external magnetic fields, which can be understood on the basis of the Bell-Bloom equation [28,29]

$$P(B_\parallel, B_\perp) = P_\infty \frac{1 + (\omega_\parallel/\gamma_2)^2}{1 + (\omega_\parallel/\gamma_2)^2 + \omega_\perp^2/\gamma_1\gamma_2}, \tag{3}$$

In this equation, $\omega_\parallel$ and $\omega_\perp$ are Larmor frequencies, where $\omega = \frac{egB}{2m} = \gamma B$ (γ is the gyromagnetic ratio), B is the magnitude of the magnetic field, and g is the g factor; $\gamma_{1,2} = \Gamma_{\mathrm{pump}} + \Gamma_{1,2}$ are effective spin relaxation rates, where Γ_{pump} is the optical pump rate and $\Gamma_{1,2}$ are the longitudinal and transverse relaxation rates, respectively; and P_∞ is the polarization ratio of atoms obtained for $B_0 \to \infty$. Under the practical conditions of the experiment, because of the existence of a residual magnetic field in the laboratory room (B_L), the longitudinal external magnetic field includes the applied magnetic field $\vec{B_0}$ and the parallel component $B_{L\parallel}$ of B_L, whereas the transverse external magnetic field is the perpendicular component $B_{L\perp}$ of B_L.

III. RESULTS AND DISCUSSION

A. Trapping of $^{84-87}$Rb isotopes

A detailed description of the trapping method as well as preliminary results of the stopping position of $^{84-87}$Rb atoms in He II were presented in a recent article [22]. During the experiment, we counted the number of injected ions and emitted LIF photons from laser-excited atoms for each degrader thickness. From the degrader thickness, we calculated the corresponding stopping position of atoms in He II using the LISE++ program, as described in Ref. [22]. Here, the finally obtained trapping results are shown in Fig. 3 as the relation between the ratio of the number of detected LIF photons N_L to the number of injected beams N_B and the stopping position of atoms in He II. The scales of the horizontal axes are closely related to the energy of each ion beam. Owing to the different energy of each ion beam, the adjustable range of the degrader thickness for the secondary ^{84,86}Rb beams is smaller than that for the primary ^{85,87}Rb beams because the secondary beam energy is lower than the primary beam energy. In Fig. 3, we can clearly identify the stopping region of atoms from the peak, although a small number of data points are plotted because only a few discrete values of degrader thickness were used in the measurement. The position of the peaks ($x = 0$) indicates that atoms were stopped along the laser path. The FWHM of the peaks is about 1 mm for ^{85,87}Rb and 0.8 mm for ^{84,86}Rb, as marked in Fig. 3, which is reasonably consistent with the

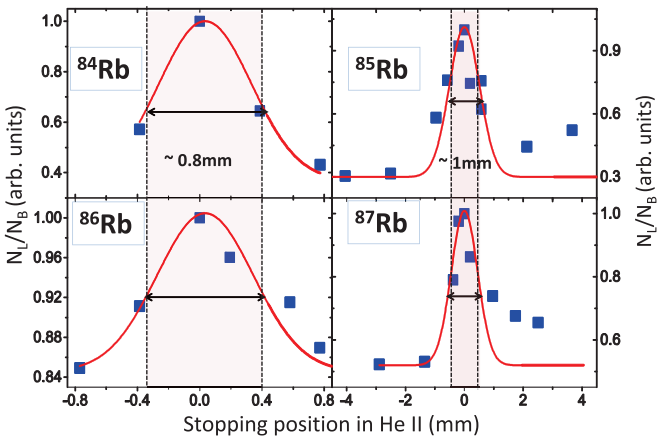

FIG. 3. (Color online) Trapping results for $^{84-87}$Rb isotopes in He II shown by the relation between the ratio of the number of detected laser-induced fluorescence photons N_L to the number of injected beams N_B and the stopping position of atoms in He II. Here, the stopping position was calculated from the thickness of the energy degrader using the LISE++ program, as described in detail in Ref. [22]. The peak position ($x = 0$) suggests the perfect overlap of the laser beam and the trapped atoms. All the Y axes are normalized by the maximum number of counts. The scales of the horizontal axes are closely related to the degrader thickness, as explained in the text.

width (about 1 mm) of the profile of the laser beam with 2.0 mm diameter. Therefore, using this trapping method, $^{84-87}$Rb ion beams were precisely trapped in the observation region of He II (typical volume: $5\times2\times2$ mm^3).

B. Spin polarization and LRDR spectra of $^{84-87}$Rb isotopes

Using the measurement pattern presented in Fig. 2, we observed the LRDR spectra of $^{84-87}$Rb isotopes. As an example, the observed spectrum for ^{87}Rb is presented in Fig. 4(a). After changing the time parameter on the horizontal axis to the applied scanning magnetic field, the LRDR spectra obtained for the Zeeman transitions of $^{84-87}$Rb in He II are shown in Fig. 4(b). In the case of ^{86}Rb, to reduce the effect of the number fluctuation of atoms in the observation region, the recording time for one cycle was changed from 10 s to 1 s. Additionally, the LRDR peak intensity for ^{86}Rb is relatively small, which is considered reasonable because the small resonance signal for the ^{86m}Rb isomer is invisible as a result of the small isomer production ratio, the fluctuation of the background count, and the number of atoms during the measurement cycle.

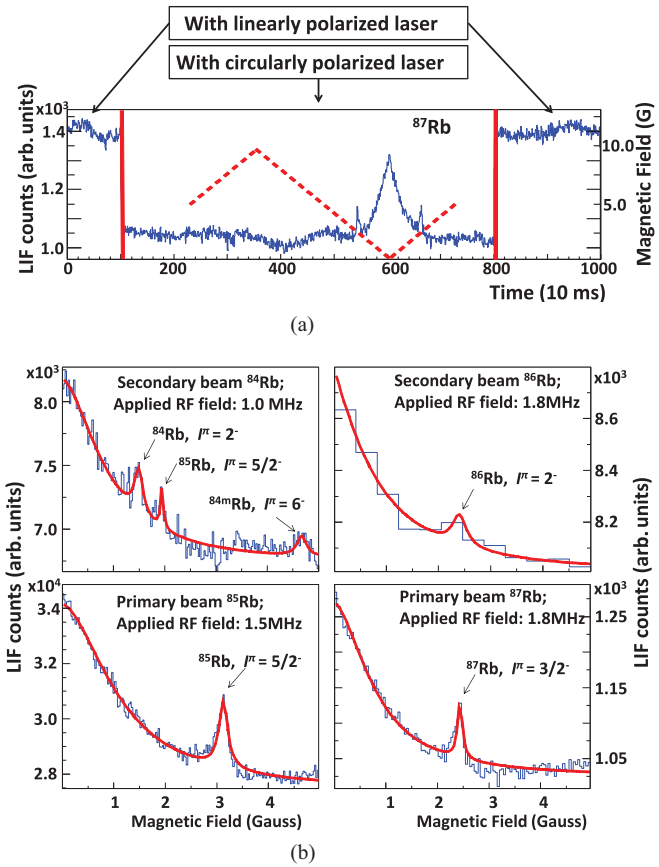

FIG. 4. (Color online) (a) Directly observed LRDR spectra, as explained in Fig. 2(b). The red dashed line is the applied magnetic field. (b) LRDR spectra of $^{84-87}$Rb, presented as the relation between the intensity of the laser-induced fluorescence photon and the scanned magnetic field B_0. The red solid line shows the fitting using Eq. (6) and a Lorentz function.

By observing the difference in the LIF intensity between the linearly and circularly polarized laser, as shown in Fig. 4(a), it is possible to evaluate the degree of polarization of the observed atoms. The polarization for each isotope achieved in the current experiment is approximately 35–40%, which is reasonable compared with the results of off-line experiments but smaller than those of other elements (Cs, Ag, and Au) [18]. The slight overlap of the D_1- and D_2-excitation spectra of Rb atoms in He II [15] should be responsible for the small polarization, as explained in Refs. [14,23]. We also suspect that several factors related to the experimental system can affect the polarization of atoms. For example, the pumping laser might be subjected to birefringence because it must traverse four cryostat windows before interacting with trapped atoms. The incompletely circularly polarized laser (up to 85% in the present experiment) also limits the polarization of observed atoms.

C. Determination of nuclear spins for $^{84-87}$Rb

Conventionally, nuclear spins can be deduced directly from the LRDR spectra using the following simplified version of Eq. (2):

$$I = \frac{\mu_B B}{\nu} - \frac{1}{2}, \tag{4}$$

which applies to the case of the ground state of an alkali-metal atom ($J = 1/2$). In this equation, ν is the the RF frequency. However, in practice, because the LRDR spectra are observed in a weak external magnetic field (<10 gauss), the residual magnetic field B_L might affect the precision of experimental results.

The effect of residual magnetic fields has been confirmed by off-line experiments, as discussed in a recent article [30]. The residual magnetic field degrades the accuracy of nuclear spins determined directly from measured LRDR signals. Therefore, to confirm the positions of resonance peaks, we have found a way to estimate B_L using the characteristics of the B_0 peak. A brief explanation of the estimation of B_L is as follows.

As we discussed in Sec. II C, Eq. (3) describes optical pumping in a longitudinal and transverse external magnetic field, whereas Eq. (1) gives the relation between emitted LIF photons and atomic polarization during optical pumping. Therefore, the observed LIF intensity for a peak around $B = 0$ can be described by combining Eqs. (1) and (3) as follows:

$$I_{\mathrm{LIF}} = I_0\left(1 - P_z \frac{1+(\gamma B_\parallel/\gamma_2)^2}{1+(\gamma B_\parallel/\gamma_2)^2+[(\gamma B_\perp)^2/\gamma_1\gamma_2]}\right). \tag{5}$$

Here, I_0 is the LIF intensity observed using a linearly polarized laser, P_z is the achieved polarization of atoms, and γ is the gyromagnetic ratio. In our experiment, the magnitude of γ_1 is estimated to be on the order of 10^4 in the limit of $\Gamma_{\mathrm{pump}} \gg \Gamma_1$, where the optical pumping rate is estimated from the photon-absorption cross section of atoms in He II. From the width of the LRDR line, after consideration of the effect of the field inhomogeneity on the width, γ_2 is on the order of 10^4–10^5. Under the current experimental conditions, $B_{L\perp}$ is roughly estimated to be 1 G. Therefore, it was ascertained that $(\gamma B_\perp)^2/\gamma_1\gamma_2$ is significantly larger than 1 (for a Rb atom, the gyromagnetic ratio γ is on the order of 10^6), meaning that

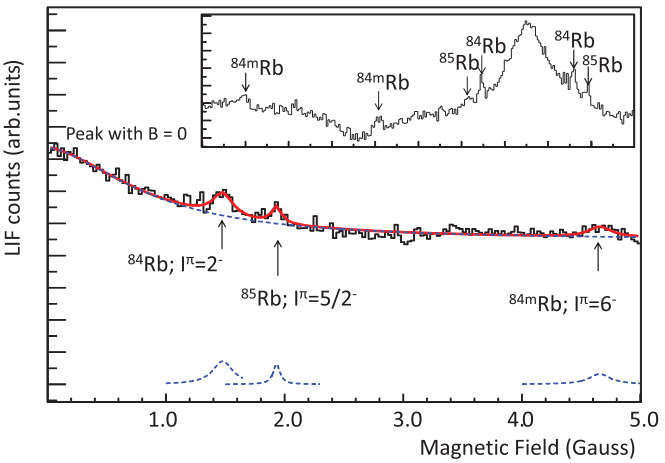

FIG. 5. (Color online) LRDR for ^{84,85}Rb isotopes and isomer ^{84m}Rb. The inset shows the directly recorded spectrum using the measurement pattern presented in Fig. 2(b).

Eq. (5) can be approximated as

$$I_{\mathrm{LIF}} = I_0\left(1 - P_z \frac{(B_\parallel - B_{L\parallel})^2}{(B_\parallel - B_{L\parallel})^2 + \frac{\gamma_2}{\gamma_1}(B_{L\perp})^2}\right) \qquad (6)$$

after taking $B_{L\parallel}$ into account. This simplified function gives a value only slightly different from the original Eq. (5) when the scanned magnetic field B approaches zero ($B \to 0$). Information on B_L ($B_{L\parallel}$ and $B_{L\perp}$) as well as the polarization of atoms is included in Eq. (6). Therefore, we can estimate the residual magnetic field by fitting the B_0 peak using Eq. (6) with a reasonable value of γ_2/γ_1 estimated from the pumping rate in the current experiment, the width of the LRDR peak, and early off-line test results. However, other factors might affect the fitting results, such as the number instability of atoms in the observation region, which slightly deforms the shape of B_0 peaks. Consequently, taking into account all possible factors, we estimated that $B_{L\parallel}$ is approximately 0.1 G and $B_{L\perp}$ is approximately 0.8 G (about ±0.1 G difference from the spectrum of each isotope), consistent with the results obtained using a gauss meter before and after the experiment.

The nuclear spin values are analyzed in the following manner. Figure 5 shows the LRDR spectra of ^{84,85}Rb. LRDR can be confirmed from the directly recorded spectrum, as presented in the inset of Fig. 5 where the peaks for one isotope appear in pairs at the same magnetic field magnitude (B_{RF}). From the inset, a pair of resonance peaks located at the side of a large magnetic field are visible in spite of the unstable LIF intensity. By comparing the deduced spin value with that from Ref. [31], this pair of peaks are identified as the Zeeman resonance for isomer ^{84m}Rb with a reasonable level of confidence. By showing the spectrum with the parameter of the magnetic field as the horizontal ordinate, three resonance peaks assigned to ^{84,84m,85}Rb can be observed clearly. After eliminating the effect of B_L estimated by fitting the peak at $B = 0$ with Eq. (6) (red solid line in Fig. 5), the nuclear spins are assigned to the three resonance peaks.

The nuclear spin values for all isotopes studied in this work, after eliminating the effect of $B_{L\parallel}$, were finally determined as presented in Table I. Several sources of experimental error must be considered here. The inaccuracy of the applied magnetic field strength is presumed to be the main component of the experimental error. About 3.3% of the error originates from the field inhomogeneity within the observation region ($5\times2\times2$ mm^3) and the uncertainty (±1 mm) of the observation region. The experimental errors determined for nuclear spins after considering all the factors are also presented in Table I. Consequently, the nuclear spin values determined in this work are consistent with the values reported in the literature within the experimental error [31,32].

TABLE I. Nuclear spins for $^{84m,84-87}$Rb determined in this work. The experimental errors for the spin values are discussed in detail in the text.

Isotopes	This work	Literature value	Ref.
^{84}Rb	1.9(1)	2^-	[31]
^{84m}Rb	6.2(2)	6^-	[31,32]
^{85}Rb	2.5(1)	$5/2^-$	[31]
^{86}Rb	1.9(2)	2^-	[31]
^{87}Rb	1.53(6)	$3/2^-$	[31]

D. Discussion and conclusion

The trapping efficiency and the detectable number of LIF photons from one injected atom are estimated from the experiment reported in this paper. In principle, using He II as the stopping medium, all introduced ions can be trapped within a limited region (~1 mm) in He II with a volume of $\pi\times5\times5\times1$ mm^3 (ion beam spot size: $\phi \approx 10$ mm). Owing to the limitation of the observation volume ($5\times2\times2$ mm^3) for the detection of the LIF, slightly more than 20% of the trapped atoms were used for laser spectroscopy measurement. In this experiment, the beam intensity (on the order of 10^4 ions/s) was synchronously counted by PL1 prior to the beam being introduced into He II. From the ratio of the number of LIF photons detected with the present experimental setup to the number of injected atoms, the number of LIF photons detected from one atom is estimated to be approximately 0.2–0.3. It is worth emphasizing that this estimation includes the losses associated with the beam transport, the trapping efficiency (>20%), the trapping time (typically 0.5 s in the current setup), the number fluctuation of atoms related to the slight convection of He II, the efficiency of the photodetection system (0.1%) including the acceptance of LIF detection (2%) [23] and the photon loss by the window of the cooling system for the PMT, the possible misalignment of the trapped region of the atoms and the irradiation region of the laser and the observation region of LIF, and so forth.

On the basis of these experimental efficiencies, the required minimum beam intensity was estimated to be 10^3 ions/s from the photon-absorption cross section of Rb atoms in He II [17]. The sensitivity of 10^3 ions/s, as discussed in Ref. [23], is predominantly limited by the background counts for photon detection arising from the large amount of stray laser light and the present experimental efficiency. The stray laser light is expected to be suppressed by upgrading the detection system by employing monochromators.

In the present study, using condensed He II, we were able to trap energetic radioactive ion beams ($^{84-87}$Rb) provided by the the RIPS. The trapping volume was precisely confirmed by laser spectroscopy. Compared with existing trapping techniques used for energetic radioactive ion beams [33,34], this method has relatively high trapping efficiency. Using this trapping method, various atomic species produced from a nuclear reaction can be introduced into He II, which cannot be achieved using conventional methods (e.g., laser sputtering [5]) employed in early studies. The trapped RI atoms are expected to be applied to various measurements in the future, such as systematic measurement of the absorption and emission spectra of various isotopes (e.g., francium) in He II. In addition, the number of atoms used for laser spectroscopy observation can be estimated from the number of ions introduced into He II. This number is important for experimental estimation of the photon-absorption cross section, which may elucidate the nature of the broadened absorption spectra of atoms in He II.

We also obtained large polarization for not only the stable isotopes but also the radioactive isotopes by optical pumping. We consider that the high polarization of RI atoms in He II has the potential to be applied to spin-related studies, such as β-decay asymmetry measurement (β-NMR experiments) of short-lived nuclei [11,27]. At present, only a few elements have been polarized by the optical pumping method, which will hinder the application of this technique. However, taking advantage of the broadened absorption spectra and long spin relaxation time of atoms in He II, it will be possible to polarize more atomic species by optical pumping, as confirmed experimentally for group 11 elements (Ag, Au) [18]. Investigation of the spin relaxation time of various atoms will also be necessary to understand the spin relaxation mechanism of atoms in He II, which will be helpful for the above-mentioned spin-related research.

In this study, LRDR spectra for stable isotopes (^{85,87}Rb), radioactive isotopes (^{84,86}Rb), and an isomer (^{84m}Rb) in He II have been observed successfully. Further observation of the laser microwave double-resonance (LMDR) spectra of RI atoms in He II is also necessary and planned to enable systematic measurement of the hyperfine constant [14]. Measurement of the LMDR and LRDR of various isotopes in He II will lead to a better understanding of the interaction between the electrons of atoms and surrounding He atoms [17], and may also provide us with some information about nuclear properties. Improvement of the experimental efficiency and the suppression of scattered laser light are also ongoing to enable this method to be applied to the measurement of RI atoms with a low yield.

IV. SUMMARY

In this work, we have presented the effective trapping and laser spectroscopy measurements of $^{84-87}$Rb isotopes with a controllable number of atoms in He II at 1.8 K. $^{84-87}$Rb isotopes produced from the RIPS with an intensity of approximately 10^4 pps and an energy exceeding 60 MeV/u were injected into He II. Using the condensed He II as a trapping medium, almost all the injected ions were stopped and neutralized in He II. The optical pumping of $^{84-87}$Rb was achieved using a circularly polarized cw laser (with a polarization ratio of over 85%) at the wavelength of the D_1 absorption line of Rb atoms (780 nm in He II). A reasonable degree of atomic polarization of as high as 35–40% was obtained. By scanning a weak magnetic field with a fixed-frequency RF field, LRDR spectra were observed for stable ^{85,87}Rb isotopes and unstable ^{84,86}Rb isotopes as well as the isomer ^{84m}Rb in the He II matrix. By making use of the properties of B_0 peaks observed in this work, using the results of early off-line tests, the background residual magnetic field was carefully estimated and found to be consistent with the value measured by using a gauss meter prior to the experiment. The nuclear spins for the ground state of $^{84-87}$Rb and the isomer ^{84m}Rb were deduced from LRDR spectra with relatively good accuracy after eliminating the effect of B_L, and the results were in good agreement with the values given in the literature. The trapping efficiency, the number of detectable LIF photons from one atom, and the sensitivity of the experimental setup have also been discussed on the basis of the present experimental observation. This work reveals new opportunities for the study of various particles trapped in condensed helium in several fields, including atomic and nuclear physics.

ACKNOWLEDGMENTS

This experiment was performed under Program No. NP0802-RRC53 at RIBF, operated by RIKEN Nishina Center and Center for Nuclear Study (CNS), The University of Tokyo. We thank the RIKEN Ring Cyclotron staff for their cooperation during the experiment. This work was partly supported by KAKENHI (Grant-in-Aid for Scientific Research). One author (X.F.Y.) is grateful for the support she received as an International Program Associate of RIKEN and acknowledges very helpful discussions with Prof. Y. L. Ye of Peking University.

[1] H. Bauer, M. Beau, A. Bernhardt, B. Friedl, and H. J. Reyher, Phys. Lett. A **137**, 217 (1989).
[2] T. Yabuzaki, T. Kinoshita, K. Fukuda, and Y. Takahashi, Z. Phys. B **98**, 367 (1995).
[3] B. Tabbert, H. Gunther, and G. zu Putlitz, J. Low Temp. Phys. **109**, 653 (1997).
[4] P. Moroshkin, A. Hofer, and A. Weis, Phys. Rep. **469**, 1 (2008).
[5] A. Fujisaki, K. Sano, T. Kinoshita, Y. Takahashi, and T. Yabuzaki, Phys. Rev. Lett. **71**, 1039 (1993).
[6] S. I. Kanorsky, M. Arndt, R. Dziewior, A. Weis, and T. W. Hansch, Phys. Rev. B **49**, 3645 (1994).
[7] S. I. Kanorsky, M. Arndt, R. Dziewior, A. Weis, and T. W. Hansch, Phys. Rev. B **50**, 6296 (1994).
[8] S. Lang, S. Kanorsky, T. Eichler, R. Müller-Siebert, T. W. Hänsch, and A. Weis , Phys. Rev. A **60**, 3867 (1999).

[9] M. Arndt, S. I. Kanorsky, A. Weis, and T. W. Hansch, Phys. Lett. A **174**, 298 (1993).
[10] D. Nettels, R. Muller-Siebert, and A. Weis, Appl. Phys. B **77**, 753 (2003).
[11] N. Takahashi, T. Shigematsu, S. Shimizu, K. Horie, Y. Hirayama, H. Izumi, and T. Shimoda, Physica B **284–288**, 89 (2000).
[12] S. A. Lyon, Phys. Rev. A **74**, 052338 (2006).
[13] T. Furukawa, Y. Matsuo, A. Hatakeyama, Y. Fukuyama, T. Kobayashi, H. Izumi, and T. Shimoda, Phys. Rev. Lett. **96**, 095301 (2006).
[14] T. Kinoshita, Y. Takahashi, and T. Yabuzaki, Phys. Rev. B **49**, 3648 (1994).
[15] Y. Takahashi, K. Sano, T. Kinoshita, and T. Yabuzaki, Phys. Rev. Lett. **71**, 1035 (1993).
[16] Y. Kato, T. Furukawa, Y. Matsuura *et al.*, RIKEN Accel. Prog. Rep. **44**, 242 (2011).
[17] T. Furukawa, Ph.D. thesis, Osaka University, 2007.
[18] T. Furukawa, Y. Matsuo, A. Hatakeyama *et al.*, Physica E **43**, 843 (2011).
[19] T. Furukawa, Y. Matsuo, A. Hatakeyama *et al.*, Hyperfine Interact. **196**, 191 (2010).
[20] T. Kubo and M. Ishihara, Nucl. Instrum. Methods B **70**, 309 (1992).
[21] X. Yang, T. Furukawa, T. Wakui *et al.*, Nucl. Instrum. Methods B **317**, 599 (2013).
[22] X. Yang, T. Furukawa, T. Wakui *et al.*, EPJ Web Conf. **66**, 11041 (2014).
[23] T. Furukawa, T. Wakui, X. Yang *et al.*, Nucl. Instrum. Methods B **317**, 590 (2013).
[24] K. Imamura, T. Furukawa, T. Wakui *et al.*, Nucl. Instrum. Methods B **317**, 595 (2013).
[25] A. Sasaki, S. Hoshino, T. Wakui *et al.*, RIKEN Accel. Prog. Rep. **42**, 193 (2009).
[26] O. Tarasov and D. Bazin, Nucl. Instrum. Methods B **266**, 4657 (2008).
[27] T. Shimoda, H. Miyatake, S. Mitsuoka *et al.*, Nucl. Phys. A **588**, c235 (1995).
[28] M. Arndt, S. I. Kanorsky, A. Weis, and T. W. Hansch, Phys. Rev. Lett. **74**, 1359 (1995).
[29] N. Castagna and A. Weis, Phys. Rev. A **84**, 053421 (2011).
[30] X. Yang, T. Furukawa, T. Fujita, K. Imamura, and Y. Matsuo, Hyperfine Interact. **227**, 147 (2014).
[31] C. Thibault, F. Touchard, S. Buttgenbach *et al.*, Phys. Rev. C **23**, 2720 (1981).
[32] V. M. Mazur, Z. M. Bigan, and D. M. Symochko, J. Phys. G: Nucl. Part. Phys. **37**, 035101 (2010).
[33] P. Mueller, I. A. Sulai, A. C. C. Villari *et al.*, Phys. Rev. Lett. **99**, 252501 (2007).
[34] A. Takamine, M. Wada, K. Okada *et al.*, Phys. Rev. Lett. **112**, 162502 (2014).